Supplementary Material for Yu et al.

Legends of supplemental figures

Figure S1. Characterization of *nrpd1* and *nrpd2* alleles. (A) Expressing *NRPD1* and *NRPD2* in *nrpd1-8 hen1-2* and *nrpd2-16 hen1-2*, respectively, restores the levels of miRNAs to those in *hen1-2*. (B) AtSN1 and cluster 2 siRNAs are absent in *nrpd1 hen1-2* and *nrpd2 hen1-2*. L*er*, the wild-type control for *hen1-2*; *nrpd1 hen1-2*, *nrpd1-8 hen1-2*; *nrpd2 hen1-2*, *nrpd2-16 hen1-2*; *nrpd1 hen1-2+NRPD1*, an *nrpd1-8 hen1-2* mutant harboring *NRDP1* genomic DNA. *nrpd2 hen1-2 +NRPD2*, a *nrpd2-16 hen1-2* mutant harboring *NRPD2* genomic DNA. RNAs were extracted from inflorescences, separated on a 15% polyacrylamide gel and probed for miR167 and miR173. The ethidium-bromide stained tRNA region of the gel is shown below to indicate the amount of RNAs used.

Figure S2. Characterization of the L1-derived *hen1-8* allele. The L1 line carries a tandem repeat of a 35S-GUS transgene silenced by PTGS. Screening the L1 mutagenized library for plants exhibiting high GUS activity allowed the identification of PTGS-deficient mutants, including *hen1-4*. Rescreening the L1 mutagenized library for plants exhibiting miRNA-related developmental phenotypes allowed the identification of mutants that support GUS silencing but have defects in the miRNA pathway, including *hen1-8*. (A) *hen1-8* exhibits similar miRNA impairment as the strong *hen1* alleles *hen1-4* and *hen1-5* in Col. Filter hybridization shows that miRNAs accumulate at similarly low levels in

hen1-4, *hen1-5* and *hen1-8* relative to L1. (B) *hen1-8* does not efficiently suppress PTGS of the L1 locus. Filter hybridization shows that GUS mRNAs accumulate at similarly low levels in L1 and *hen1-8* whereas they accumulate at high levels in *hen1-4*. GUS activities, as measured from plant extracts, correlate with GUS mRNA levels. (C) *hen1-8* does not affect PTGS triggered by the cucumber mosaic virus (CMV). Hypersusceptibility to CMV infection is a hallmark of PTGS-deficient mutants and correlates with increased accumulation of viral RNA due to the impairment of the PTGS antiviral defense, which leads to the eventual death of the infected plant. Consistent with its ability to undergo transgene PTGS, *hen1-8* mutants exhibit CMV tolerance, whereas *hen1-4* exhibits CMV hypersusceptibility.

Figure S3. Levels of HEN1 protein do not differ between L*er* and Col backgrounds. Total proteins from L*er* and Col inflorescences were resolved by SDA-PAGE and transferred to a nitrocellulose membrane. The top and bottom halves of the membrane were probed with anti-HEN1 and anti-Hsp73 (mouse monoclonal antibody) antibodies, respectively. The anti-Hsp73 antibody detects *Arabidopsis* Hsp70 proteins, which serve as a loading control. A portion of the stained protein gel is shown at the bottom.

Table S1. The relative abundance of rare miRNAs in *rdr2-1* and WT

	rdr2-1[a]	WT[a]	Fold change[b]
miR771	5.2E-05	1.0E-04	0.5
miR773	1.6E-05	1.3E-05	1.2
miR774	3.2E-06	N/A[c]	
miR775	7.5E-04	1.9E-04	4
miR776	4.3E-06	N/A	
miR777	5.0E-05	N/A	
miR778	5.3E-06	N/A	
miR779	1.1E-06	N/A	
miR780	2.2E-03	3.4E-04	6.4
miR781	2.0E-05	N/A	
miR822	1.1E-05	6.3E-06	1.7
miR823	1.4E-05	6.3E-06	2.2
miR824	1.4E-03	8.2E-05	17.4
miR825	5.4E-05	3.1E-05	1.7
miR826	5.4E-06	N/A	
miR827	5.5E-05	1.7E-04	0.3
miR829	2.0E-03	1.1E-03	1.7
miR830	2.0E-05	N/A	
miR832	2.1E-06	N/A	
miR835	3.2E-06	N/A	
miR837	1.1E-06	N/A	
miR838	1.2E-05	N/A	
miR839	9.6E-06	7.0E-05	0.1
miR840	1.9E-05	6.3E-06	3.0
miR844	2.1E-05	6.3E-06	3.4
miR845a	1.7E-04	1.3E-05	13.1
miR845b	1.8E-05	N/A	
miR848	2.8E-04	1.3E-05	21.3
miR851	4.8E-05	1.9E-05	2.5
miR852	6.2E-05	6.3E-06	9.7
miR853	1.1E-06	N/A	
miR856	N/A	6.5E-06	
miR858	6.7E-05	7.0E-05	1.0
miR860	5.1E-05	1.9E-05	2.7
miR861	7.4E-06	N/A	
miR862	1.1E-05	6.3E-06	1.7
miR864	6.5E-05	1.9E-05	3.4
miR865	1.1E-06	N/A	
miR866	1.2E-04	3.2E-05	3.8
miR867	2.6E-04	6.3E-06	41.0
miR869	2.1E-04	3.8E-05	5.6

a: The relative abundance was calculated as: individual miRNA count/total miRNA count
b: Fold change was calculated as: relative miRNA abundance of *rdr2-1*/relative miRNA abundance of wt
c: N/A, undetected.

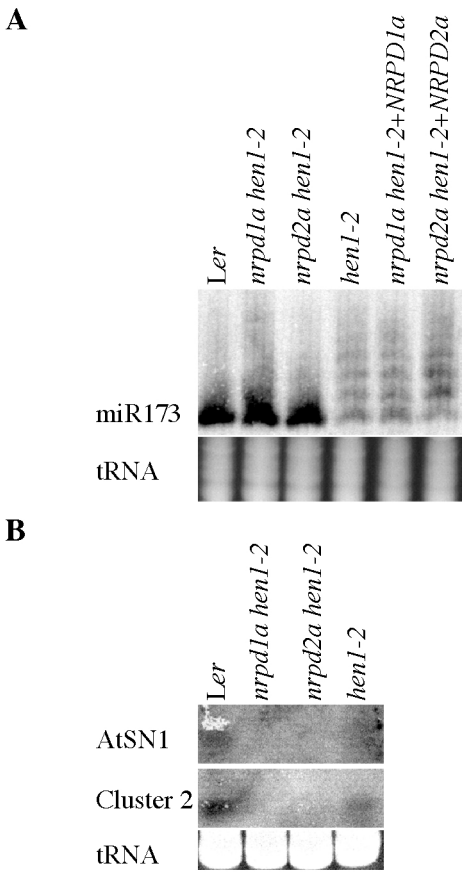
A
Ler
nrpd1a hen1-2
nrpd2a hen1-2
hen1-2
nrpd1a hen1-2+NRPD1a
nrpd2a hen1-2+NRPD2a
miR173
tRNA
B
Ler
nrpd1a hen1-2
nrpd2a hen1-2
hen1-2
AtSN1
Cluster 2
tRNA

Figure S1

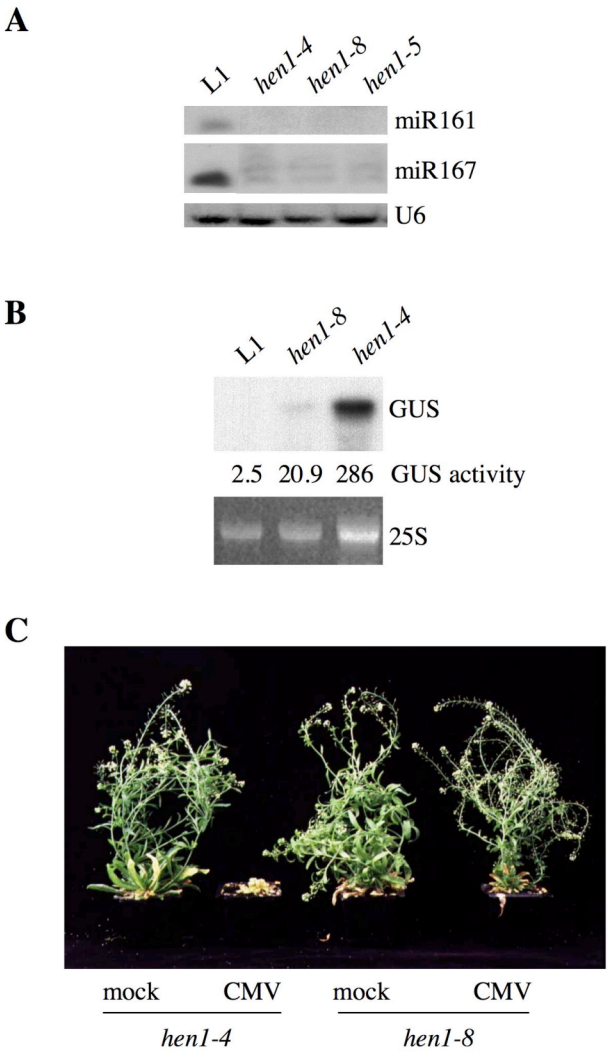
A
L1
hen1-4
hen1-8
hen1-5
miR161
miR167
U6
B
L1
hen1-8
hen1-4
GUS
2.5 20.9 286 GUS activity
25S
C
mock
CMV
mock
CMV
hen1-4
hen1-8

Figure S2

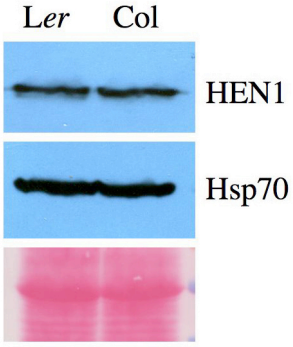

Figure S3